The current issue and full text archive of this journal is available at
www.emeraldinsight.com/0961-5539.htm

Combined effect of radiation and natural convection in a rectangular enclosure discreetly heated from one side

A. Bahlaoui and A. Raji
Unit of Formation and Research of Chemistry and Sciences of the Environment, Faculty of Sciences and Techniques, Beni-Mellal, Morocco, and

M. Hasnaoui
Unit of Formation and Research of Thermics and Fluid Mechanics, Department of Physics, Faculty of Sciences Semlalia, Marrakech, Morocco

Received July 2004
Revised May 2005
Accepted July 2005

Abstract

Purpose – The aim of this work consists of studying numerically the coupling between natural convection and radiation in a tall rectangular cavity by examining the effect of the emissivity of the walls, ε, the Rayleigh number, *Ra*, and the inclination of the cavity, θ, on the flow characteristics and the existence ranges of the multiple solutions obtained.

Design/methodology/approach – The Navier-Stokes equations were discretized by using a finite difference technique. The vorticity and energy equations were solved by the alternating direction implicit method. Values of the stream function were obtained by using the point successive over-relaxation method. The calculation of the radiative heat exchange between the walls of the cavity is based on the radiosity method.

Findings – For an inclined cavity ($\theta = 45°$), up to four different solutions are obtained and their range of existence is found to be strongly dependent on the Rayleigh number and the emissivity of the cavity walls. In the case of a vertical cavity ($\theta = 90°$), the weak reduction of the convection effect due to radiation is largely compensated for by the contribution of the radiation which enhances the overall heat transfer through the cold surface of the cavity and favours the appearance of secondary cells.

Originality/value – The existence of multiple steady-state solutions in an inclined cavity ($\theta = 45°$) and the number of the obtained solutions are affected by the presence of radiation. In face, the increase of the emissivity reduces the number of solutions for weak values of the Rayleigh number. Also, the increase of this parameter favours the multiplicity of solutions for all the considered values of the emissivity. For a vertical cavity ($\theta = 90°$), the effect of radiation generates an oscillatory convection for large values of the Rayleigh number.

Keywords Convection, Radiation, Discrete control systems, Numerical control, Heat transfer, Solutions

Paper type Research paper

Nomenclature

A_r = aspect ratio of the cavity $A_r = L'/H'$

F_{ij} = view factor between S_i and S_j elements

g = acceleration due to the gravity, m/s^2

H' = height of the cavity, m

I_i = dimensionless irradiation, $I_i = I'_i/\sigma T'^4_C$

J_i = dimensionless radiosity, $J_i = J'_i/\sigma T'^4_C$

International Journal of Numerical Methods for Heat & Fluid Flow
Vol. 16 No. 4, 2006
pp. 431-450

0961-5539
DOI 10.1108/09615530610653073

L' = length of the cavity, m
N_r = convection-radiation interaction parameter, $N_r = \sigma T'^4_C H'/\lambda(T'_H - T'_C)$
Nu = average Nusselt number
Pr = Prandtl number, $\mathrm{Pr} = \nu/\alpha$
Q_r = dimensionless net radiative heat flux, $Q_r = Q'_r/\sigma T'^4_C$
Ra = Rayleigh number, $Ra = g\beta(T'_H - T'_C)H'3/\alpha\nu$
t = dimensionless time, $t = t'\alpha/H'2$
T = dimensionless fluid temperature, $T = (T' - T'_C)/(T'_H - T'_C)$
T'_C = temperature of the cold wall, K
T'_H = temperature of the heated elements, K
T_o = dimensionless reference temperature, $T_o = T'_C/(T'_H - T'_C)$
(u, v) = dimensionless horizontal and vertical velocities, $(u, v) = (u', v')H'/\alpha$
(x, y) = dimensionless Cartesian coordinates, $(x, y) = (x', y')/H'$

Greek symbols
α = thermal diffusivity of the fluid, m^2/s
β = thermal expansion coefficient of the fluid, 1/K
ε = emissivity of the cavity walls
λ = thermal conductivity of fluid, W/mK
ν = kinematic viscosity of fluid, m^2/s
Ω = dimensionless vorticity, $\Omega = \Omega' H'^2/\alpha$
Ψ = dimensionless stream function, $\Psi = \Psi'/\alpha$
σ = Stéfan-Boltzman constant, $\alpha = 5,669 \times 10^{-8}\ \mathrm{W/(m^2K^4)}$
θ = inclination of the cavity (in degree)

Subscripts
C = cold surface
CR = critical
cv = convection
H = heated surface
loc = local
rd = radiation

Superscripts
′ = dimensional variable

Introduction

In the past, considerable efforts have been devoted to study natural convection flows generated by buoyancy forces in enclosures discretely heated from one side (Torrance, 1979; Refai Ahmed and Yovanovich, 1991, 1992). The interest in such problems stems from their importance in many engineering applications such as convective heat loss from solar collectors, thermal design of buildings, air conditioning, and recently, the cooling of electronic components. However, the natural convection can ensure the heat evacuation when the heat losses of the system are relatively weak. To improve the cooling process, the recourse to an external ventilation is often considered as a means to achieve higher thermal performances (Raji and Hasnaoui, 1998a, b, 2000). In applications using natural convection as a heat removal mechanism, the range of temperatures is normally low and, therefore, it would be justifiable to neglect radiation effects for both simplicity and computational economy purposes. But, in general, thermal radiation is present and its interaction with natural convection is important in diverse situations of practical interest and many engineering applications. In earlier studies of Larson and Viskanta (1976) and Kim and Viskanta (1984), coupling between radiation and natural convection was considered in closed cavities. The authors showed that the effect of radiation contributes to increase the total heat transfer in comparison with the case of pure natural convection. In addition, it was found that radiation leads to a decrease of the convective component but this decrease is largely compensated by the radiation contribution to the global heat transfer. In previous studies, the effect of radiation was also considered in the case of closed cavities uniformly heated from one side and cooled from the opposite side (Balaji and Venkateshan, 1993, 1994a; Akiyama and Chong, 1997; Ramesh *et al.*, 1999; Ramesh and

Venkateshan, 1999). These studies showed that, in addition to the limited reduction of the natural convection effect, the radiation leads to homogenise the temperature inside the cavity and supports the overall heat transfer rate evacuated through the rigid walls. Recently, a numerical study was carried out by Ridouane *et al.* (2004) on natural convection, coupled with surface radiation, in a square cavity heated from below. The results obtained show that the surface radiation reduces significantly the critical Rayleigh number characterizing the transition toward the oscillatory convection. Also, the authors show that it is possible to transit from a steady-state solution to a chaotic one by simply increasing the emissivity. Other studies were mainly centred on partially open cavities, either uniformly (Balaji and Venkateshan, 1994b) or discreetly (Dehghan and Behnia, 1995, 1996) heated. The last mode of heating is in fact encountered in several practical situations and more efforts are useful to better understand the interaction between natural convection and radiation in terms of dynamical and thermal behaviours of fluids confined in discretely heated rectangular enclosures.

The aim of this work consists to study numerically the coupling between natural convection and radiation in a tall rectangular cavity by examining the effect of the emissivity of the walls, ε, the Rayleigh number, Ra, and the inclination of the cavity, θ, on the flow characteristics and the existence ranges of the multiple solutions obtained. The attention is also focused on the contribution of each heat transfer mode (convection and radiation) to the overall heat transfer.

Problem formulation

The studied configuration is sketched in Figure 1. It consists of an inclined closed rectangular cavity with an aspect ratio $A_r = L'/H' = 10$. The cavity is discreetly heated from one side ($y' = 0$) with a constant temperature and cooled from the opposite side ($y' = H'$) with a uniform temperature, while the remaining short walls are considered adiabatic. All the inner surfaces in contact with the studied fluid are assumed to be gray, diffuse emitters and reflectors of radiation. The fluid flow is assumed to be two-dimensional and laminar, the fluid properties are independent of temperature and the assumption of an incompressible fluid obeying the Boussinesq approximation is valid. The dimensionless governing equations, written in Ω-Ψ formulation, are:

$$\frac{\partial \Omega}{\partial t} + \frac{\partial (u\Omega)}{\partial x} + \frac{\partial (v\Omega)}{\partial y} = Pr\left[\frac{\partial^2 \Omega}{\partial x^2} + \frac{\partial^2 \Omega}{\partial y^2}\right] + Ra\,Pr\left[\cos\theta \frac{\partial T}{\partial x} - \sin\theta \frac{\partial T}{\partial y}\right] \qquad (1)$$

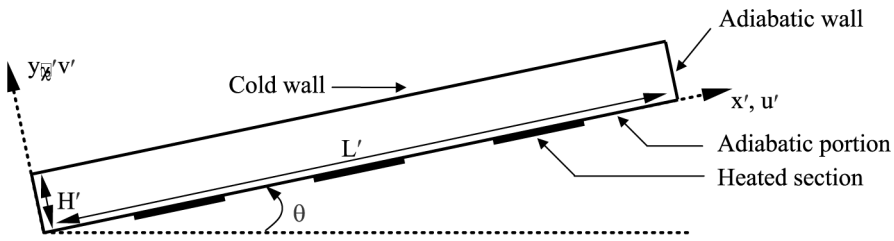

Figure 1.
Schematic of the studied configuration

$$\frac{\partial T}{\partial t}+\frac{\partial (uT)}{\partial x}+\frac{\partial (vT)}{\partial y}=\left[\frac{\partial^2 T}{\partial x^2}+\frac{\partial^2 T}{\partial y^2}\right] \tag{2}$$

$$\frac{\partial^2 \Psi}{\partial x^2}+\frac{\partial^2 \Psi}{\partial y^2}=-\Omega \tag{3}$$

and:

$$u=\frac{\partial \Psi}{\partial y}, \quad v=-\frac{\partial \Psi}{\partial x} \tag{4}$$

Boundary conditions
The boundary conditions are such as:

$u = v = \Psi = 0$ on the rigid walls

$T = 0$ on the cold wall

$T = 1$ on the heated elements

$-\frac{\partial T}{\partial n} + N_r Q_r = 0$ on the adiabatic elements

where n represents the normal direction to the considered adiabatic wall.

Radiation equations
The calculation of the radiative heat exchange between the walls of the cavity is based on the radiosity method. The grid used for convection (211 × 21) is retained for radiation and consists of a 464 isothermal elementary surfaces. The view factors between these sub-surfaces were determined by Hottel and Saroffim's (1967) crossed string method. In addition, the radiative heat transfer between the system surfaces is expressed by the following set of equations in non-dimensional form:

$$J_i-(1-\varepsilon_i)\sum_{S_j} F_{ij}J_j=\varepsilon_i\left[\frac{T_i}{T_o}+1\right]^4 \tag{5}$$

The dimensionless net radiative heat flux leaving a surface S_i is evaluated by:

$$Q_r=J_i-I_i=\varepsilon_i\left[\left(\frac{T_i}{T_o}+1\right)^4-\sum_{S_j} F_{ij}J_j\right] \tag{6}$$

Heat transfer

The average Nusselt numbers characterising the contributions of natural convection and thermal radiation through the cold wall are, respectively, defined as:

$$Nu_{cv}=-\frac{1}{A_r}\int_0^{A_r}\frac{\partial T}{\partial y}\bigg|_{y=1} dx \quad Nu_{rd}=\frac{1}{A_r}\int_0^{A_r} N_r Q_r\bigg|_{y=1} dx \tag{7}$$

The total Nusselt number, Nu, is the sum of the corresponding convective and radiative Nusselt numbers, i.e. $Nu = Nu_{cv} + Nu_{rd}$.

Numerical method

Equations (1)-(3) are discretized by using a finite difference procedure. Forward finite difference in time and central differences in space (diffusive and convective terms) are used. The integration of equations (1) and (2) was ensured by the Alternate Direction Implicit method. Values of the stream function at all grid points were obtained with equation (3) by using the point successive over-relaxation method with an optimum value of 1.8 for the over-relaxation coefficient corresponding to the grid 211 × 21 adopted in the present study. The set of equations, representing the radiative heat transfer between the different elementary surfaces of the cavity and described by equation (6), is solved by using the Gauss-Seidel method. The results of the numerical code were validated with those obtained by Akiyama and Chong (1997). Comparisons were made in terms of the convective Nusselt numbers calculated at the heated wall of a square cavity differentially heated. The comparisons, performed for Ra in the range $10^3 \leq Ra \leq 10^6$, showed a good agreement since the relative maximum deviations being less than 1.07 per cent and 1.36 per cent for $\varepsilon = 0$ and $\varepsilon = 1$,, respectively, (Table I). Other tests of validation were also performed and showed an excellent agreement with the results obtained by Ramesh *et al.* (1999) and Balaji and Venkateshan (1994c) in terms of temperature profiles along the adiabatic horizontal walls and in terms of the radiative Nusselt number. The maximum differences observed were less than 5 per cent.

Various preliminary tests were also conducted to check the dependence of the results on the grid used. It was found that a grid of 211 × 21 in x and y directions is a reasonable compromise between computational effort and required accuracy. In fact, comparison between the results obtained with this grid and finer grids of 315 × 31 and 421 × 41, showed limited quantitative differences. More precisely, the maximum deviations observed in terms of Ψ_{max} and Nu, calculated along the cold wall of the cavity, are within 1.58 per cent when comparing the results obtained with grids of 211 × 21 and 421 × 41 (Table II).

Table I.
Effect of Ra and ε on the mean convective Nusselt number, Nu_{cv}, evaluated on the heating wall of a square cavity for $T'_H = 298.5$ K and $T'_C = 288.5$ K

	$\varepsilon = 0$				$\varepsilon = 1$			
Ra	10^3	10^4	10^5	10^6	10^3	10^4	10^5	10^6
Present work	1.118	2.257	4.627	9.475	1.250	2.242	4.192	8.100
(Akiyama and Chong, 1997)	1.125	2.250	4.625	9.375	1.250	2.250	4.250	8.125

Table II.
Effect of the grid size for $\theta = 0°$, $\varepsilon = 0.5$ and various values of Ra

	$Ra = 10^4$		$Ra = 5 \times 10^4$		$Ra = 10^5$		$Ra = 5 \times 10^5$	
Grids	Ψ_{max}	Nu	Ψ_{max}	Nu	Ψ_{max}	Nu	Ψ_{max}	Nu
211 × 21	8.832	3.669	19.750	4.453	27.247	4.866	57.819	6.209
315 × 31	8.831	3.671	19.753	4.378	27.292	4.787	58.801	6.162
421 × 41	8.831	3.670	19.744	4.390	27.280	4.789	58.463	6.212

Results and discussion

Case of an inclined cavity ($\theta = 45°$)

When the inclination angle of the cavity is $\theta = 45°$, four types of solutions were obtained: a multi-cellular flow structures for which the flow is organised in three (solution of $\mathbf{S}_3$ type), five (solution of $\mathbf{S}_5$ type) or seven (solution of $\mathbf{S}_7$ type) closed cells of different size and a unicellular flow structure (solution of $\mathbf{S}_1$ type). These steady-state solutions have been obtained numerically using appropriate initial conditions. In fact, the solutions of $\mathbf{S}_1$ and $\mathbf{S}_3$ types were obtained by starting the computations with the pseudo-conductive regime (a quiescent state and a linear temperature profile, decreasing from the heated wall towards the cold one). The solution of $\mathbf{S}_5$ type requires a coupled natural convection-radiation solution as an initial condition. The solution of $\mathbf{S}_7$ type was obtained by starting the numerical computations with a pure natural convection solution ($\varepsilon = 0$) corresponding to a lower value of *Ra*. Other kinds of initial conditions, different from those mentioned, were also tried, but the final state was either one of the four obtained solutions.

Streamlines and isotherms. Typical streamlines and isotherms, illustrating the four types of solutions previously defined, are presented in Figure 2(a)-(c) for $Ra = 10^5$, $\theta = 45°$ and various values of ε. In the absence of the radiation effect, Figure 2(a), shows the solution of $\mathbf{S}_7$ type where the flow is composed of three relatively dominant cells turning in the trigonometric direction, three cells of low importance turning clockwise and a seventh cell of less importance in terms of size and intensity, turning in the trigonometric direction and whose development is affected by the existence of the confining upper adiabatic short wall. For the solution of $\mathbf{S}_5$ type, the trigonometric flow occupies the lower half part of the cavity while the remaining four cells are comparable to those described for $\mathbf{S}_7$ and located in the upper half of the cavity. The corresponding isotherms are marked by the presence of an important heat exchange between the heating elements and the fluid and also between the cold surface and the ascending fluid which provides from two counter-rotating cells. In the case of the solution of $\mathbf{S}_1$ type, the streamlines illustrate the presence of a large closed cell occupying the whole space offered in the cavity. The isotherms corresponding to the unicellular flow show important temperature gradients at the level of the heating elements and in the vicinity of the upper right corner, where the heat exchange is important between the heated fluid and the cold surface. For the same value of *Ra*, when the effect of radiation is considered ($\varepsilon = 0.7$), the solutions of $\mathbf{S}_5$ and $\mathbf{S}_7$ types persist (Figure 2(b)) while the unicellular flow (solution of $\mathbf{S}_1$ type) disappears by transiting towards a solution of $\mathbf{S}_3$ type after a window of periodicity, observed in a small range of ε between 0.3 and 0.4. For this latter solution, the flow is formed by a dominant cell, rotating in the trigonometric direction, occupying a great part of the space offered inside the cavity and two other small cells in the remaining space. The corresponding isotherms show that the heat transfer through the cold surface is important in the upper part of the cavity. For $\varepsilon = 1$, the only remaining solution is that of $\mathbf{S}_7$ type which is presented in Figure 2(c). If we except the visible weakness of the small extreme cell, the effect of the emissivity remains qualitatively limited on the flow structure and temperature distribution inside the cavity. It can be deduced from the preceding that the number of obtained solutions is reduced by increasing ε and the disappearance of solutions of $\mathbf{S}_3$ and $\mathbf{S}_5$ types is observed from critical values of ε which are given in the next section.

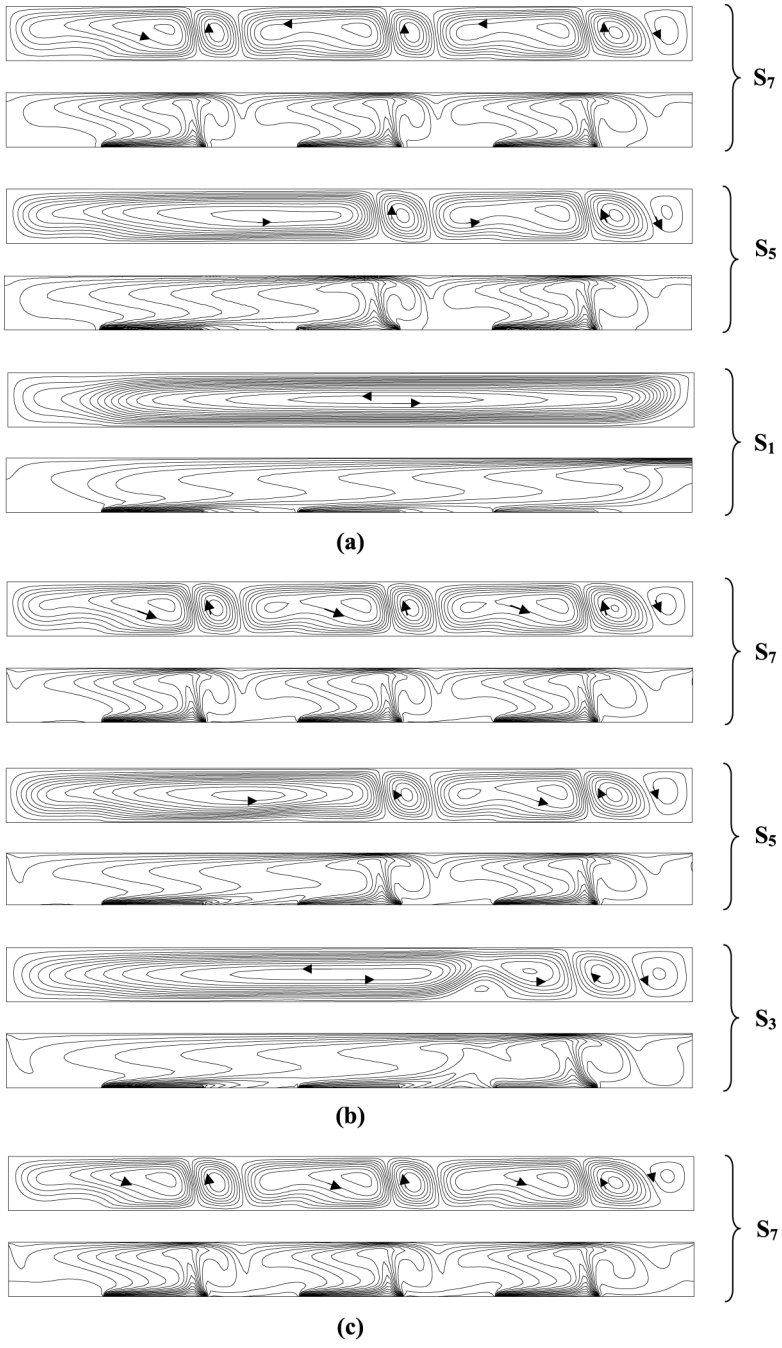

Figure 2.
Streamlines and isotherms in the case of solutions of $\mathbf{S}_1$, $\mathbf{S}_3$, $\mathbf{S}_5$ and $\mathbf{S}_7$ types, obtained for $Ra = 10^5$, $\theta = 45°$ and various values of ε. (a) $\varepsilon = 0$ ($\mathbf{S}_1 : \Psi_{min} = -0.20$, $\Psi_{max} = 53.13$), ($\mathbf{S}_5 : \Psi_{min} = -21.08$, $\Psi_{max} = 35.27$) and ($\mathbf{S}_7 : \Psi_{min} = -20.74$, $\Psi_{max} = 22.52$); (b) $\varepsilon = 0.7$ ($\mathbf{S}_3 : \Psi_{min} = -21.44$, $\Psi_{max} = 44.69$), ($\mathbf{S}_5 : \Psi_{min} = -20.70$, $\Psi_{max} = 36.59$) and ($\mathbf{S}_7 : \Psi_{min} = -20.71$, $\Psi_{max} = 22.22$); and (c) $\varepsilon = 1$ ($\mathbf{S}_7 : \Psi_{min} = -20.85$, $\Psi_{max} = 21.71$)

Effect of ε on the Nusselt numbers.

Case of $Ra = 10^5$. Variations, with ε, of the convective, radiative and total Nusselt numbers are presented in Figure 3(a)-(c) for the different types of solutions obtained for $Ra = 10^5$ and $\theta = 45°$. It can be seen from Figure 3(a) that Nu_{cv} increases slightly with ε for values of $\varepsilon \leq 0.1$ and $\varepsilon \leq 0.3$,, respectively, for the solutions of $\mathbf{S}_5$ and $\mathbf{S}_7$ types. Above these values, the tendency is reversed but the quantitative change remains limited since the maximum relative differences between the higher and lower values of Nu_{cv}, observed by varying ε, are about 8.20 per cent and 6.65 per cent, respectively, for the solutions of $\mathbf{S}_5$ and $\mathbf{S}_7$ types. Note that, when ε reaches the critical value $\varepsilon_{CR} = 0.93$, the solution of $\mathbf{S}_5$ type transits directly towards that of $\mathbf{S}_7$ type. The solution of $\mathbf{S}_1$ type (unicellular flow) which was obtained only for low values of ε, transits towards the unsteady solution of $\mathbf{S}_3$ type from $\varepsilon = 0.3$. In fact, the nature of the flow is oscillatory periodic of $\mathbf{S}_3$ type in the range $0.3 \leq \varepsilon \leq 0.4$ (full circles in Figure 3(a)). This dynamic behaviour is justified by the change of the flow structure from unicellular to multicellular flow. Above this range of ε, the solution becomes steady. When ε reaches the value 0.71, a direct transition occurs from $\mathbf{S}_3$ towards $\mathbf{S}_5$. Also for a given ε, the most important natural convection heat transfer is obtained for $\mathbf{S}_7$ and, in general, the heat transfer by natural convection increases with the number of cells since the latter are in contact with the heating elements and the cold surface. Variations of the radiative Nusselt number are presented in Figure 3(b) where it is seen that Nu_{rd} increases in a monotonous way with ε for all the obtained solutions and the radiation effect is supported by the solutions of $\mathbf{S}_1$ and $\mathbf{S}_3$ types, respectively, for $\varepsilon < 0.3$ and $\varepsilon \geq 0.3$. In general, more important is the number of the cells, weaker is the radiation effect. For the different obtained solutions, the contribution of radiation to the total heat transfer is found to be dominant for $\varepsilon \geq 0.7$. In Figure 3(c), it is seen that the effect of radiation acts in increasing the total heat transfer for all the obtained solutions.

Case of $Ra = 2 \times 10^5$. For this value of Ra, three different solutions were obtained in the considered range of ε. In Figure 4(a)-(c), variations, with ε, of the mean convective, radiative and total Nusselt numbers are illustrated. The evolutions of Nu_{cv} in the case of solutions of $\mathbf{S}_5$ and $\mathbf{S}_7$ types, presented in Figure 4(a), are characterised first by a slight increase with ε for $\varepsilon \leq 0.2/(\leq 0.3)$ in the case of $\mathbf{S}_5/(\mathbf{S}_7)$ followed by a noticeable decrease with this parameter beyond these thresholds. In the case of the unicellular or three-cellular flows, the convective Nusselt number decreases for all the considered values of ε. The solution of $\mathbf{S}_1$ type transits towards that of $\mathbf{S}_3$ type from $\varepsilon = 0.1$. In the range $0.1 \leq \varepsilon \leq 0.7$, which is larger when compared with that of $Ra = 10^5$, the solution of $\mathbf{S}_3$ type is unsteady periodic. The oscillations obtained are of simple nature with small amplitude and period if we except Ψ_{min} whose variation with time presents relatively significant amplitudes. In addition, the three types of solutions ($\mathbf{S}_3$, $\mathbf{S}_5$ and $\mathbf{S}_7$) persist for ε beyond 0.1. The radiative heat transfer increases monotonously with ε as shown in Figure 4(b) and its contribution becomes more important to that of natural convection in the case of walls highly emissive ($\varepsilon \geq 0.7$) for all these solutions. The variation of Nu, presented in Figure 4(c), shows that the total heat flow increases with ε.

Effect of Ra *on the Nusselt numbers.*

Case of $\varepsilon = 0$. In the absence of radiation, the convective Nusselt number variations, with Ra, are presented in Figure 5 for $\theta = 45°$. For all types of solutions, these variations are characterized by a continuous increase with Ra. In addition, the solution

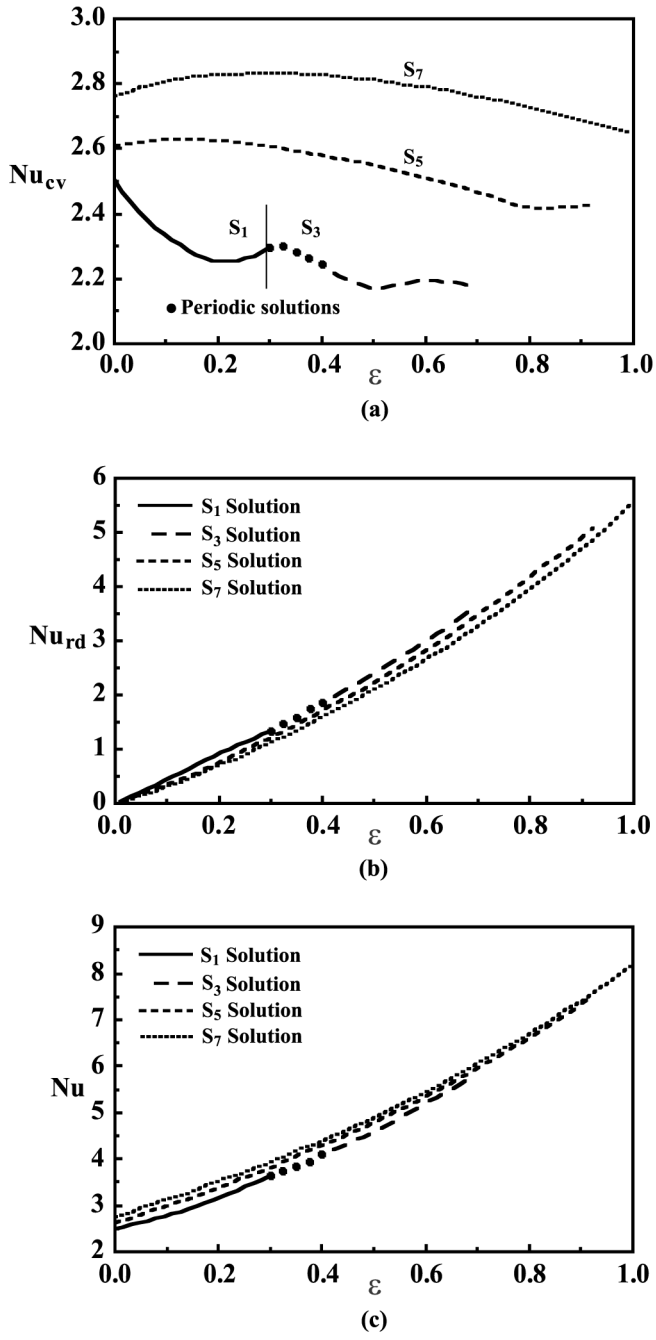

Figure 3.
Variations, with ε, of the average Nusselt numbers on the cold wall of the cavity for $Ra = 10^5$, $\theta = 45°$ and different obtained solutions. (a) Nu_{cv}; (b) Nu_{rd}; and (c) Nu

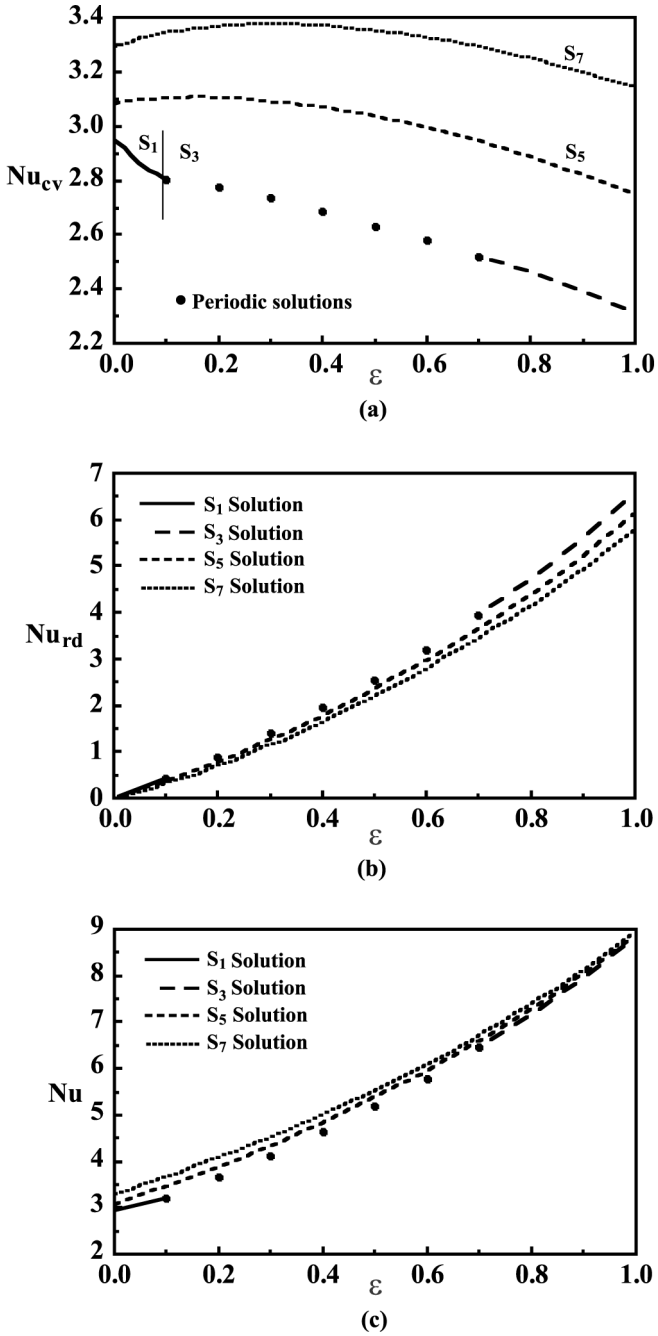

Figure 4.
Variations, with ε, of the average Nusselt numbers on the cold wall of the cavity for $Ra = 2 \times 10^5$, $\theta = 45°$ and different obtained solutions. (a) Nu_{cv}; (b) Nu_{rd}; and (c) Nu

of $\mathbf{S}_7/(\mathbf{S}_1)$ type is the most/(least) favourable to the convective heat transfer because of the corresponding multicellular/(unicellular) flow structure. The multiplicity of solutions is found to appear for values of $Ra \geq 2.8 \times 10^3$. Below this critical value of Ra, only the solution of $\mathbf{S}_1$ type was obtained. A periodic behaviour of the flow appears for great values of Ra in the case of $\mathbf{S}_5$ and $\mathbf{S}_7$; it is favoured by the multicellular nature of the flow.

Case of $\varepsilon = 0.5$. Convective, radiative and total Nusselt numbers variations with Ra are presented in Figure 6(a)-(c) for $\varepsilon = 0.5$ and $\theta = 45°$. Compared to the previous case ($\varepsilon = 0$), similar tendencies are observed in the variations of Nu_{cv} with Ra (Figure 6(a)). However, the effect of radiation is well visible and it is characterized by a delay in the appearance of solutions of $\mathbf{S}_3$ and $\mathbf{S}_5$ types, while that of $\mathbf{S}_7$ type is obtained for all the considered range of Ra. More precisely, the solution of $\mathbf{S}_3/(\mathbf{S}_5)$ type was obtained for $Ra \geq 3.1 \times 10^4/(\geq 1.9 \times 10^4)$. It is also observed that sustained oscillatory evolutions, represented by full circles in the figures, are obtained for all types of solutions at relatively high values of Ra. In Figure 6(b), the radiative heat transfer corresponding to $\mathbf{S}_7$ is characterized first by a decrease with Ra in the range $[10^3, 2 \times 10^4]$ but the tendency is inverted above this range. In addition, the solution of $\mathbf{S}_3$ type is the most favourable to the radiative heat transfer compared to the two other solutions and the importance of the radiative heat transfer decreases when the number of cells increases. The contribution of radiation to the total heat transfer is found to be dominant for $Ra \leq 10^5$, $Ra \leq 5 \times 10^4$ and $Ra \leq 2 \times 10^4$,, respectively, for the solutions of $\mathbf{S}_3$, $\mathbf{S}_5$ and $\mathbf{S}_7$ types. The variations of Nu with Ra are presented in Figure 6(c) and show similar tendencies to those observed in the variations of Nu_{cv}.

Case of $\varepsilon = 1$. When the walls of the cavity are highly emissive, the multiplicity of solutions is observed at higher values of Ra; which means that the increase of the emissivity acts in delaying the appearance of the solutions of $\mathbf{S}_3$ and $\mathbf{S}_5$ types. Hence, for $\theta = 45°$ and $\varepsilon = 1$, the solution of $\mathbf{S}_3/(\mathbf{S}_5)$ type is obtained in a small range of Ra starting from $1.5 \times 10^5/(1.2 \times 10^5)$. The variations, with Ra, of Nu_{cv}, presented in Figure 7(a), are characterized by a continuous increase of the convective Nusselt number with Ra for the solution of $\mathbf{S}_7$ type and the latter is obtained in the whole considered range of Ra. In the case of the radiative Nusselt number, Figure 7(b) shows that the increase of Nu_{rd} with Ra becomes significant especially for $Ra > 10^5$. A quantitative comparison of the heat transfer resulting from convection and radiation

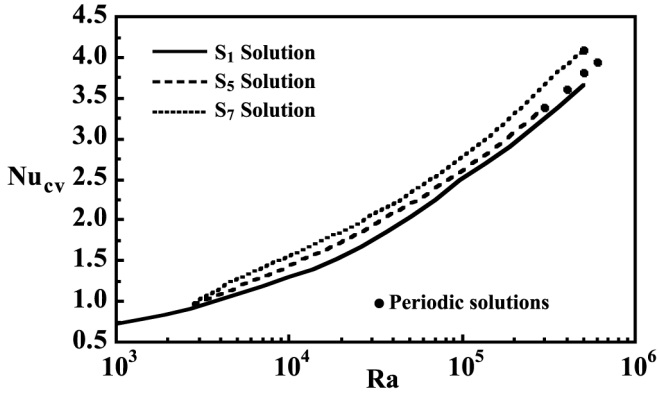

Figure 5.
Variations, with Ra, of the average convective Nusselt number on the cold wall of the cavity for $\varepsilon = 0$, $\theta = 45°$ and different obtained solutions

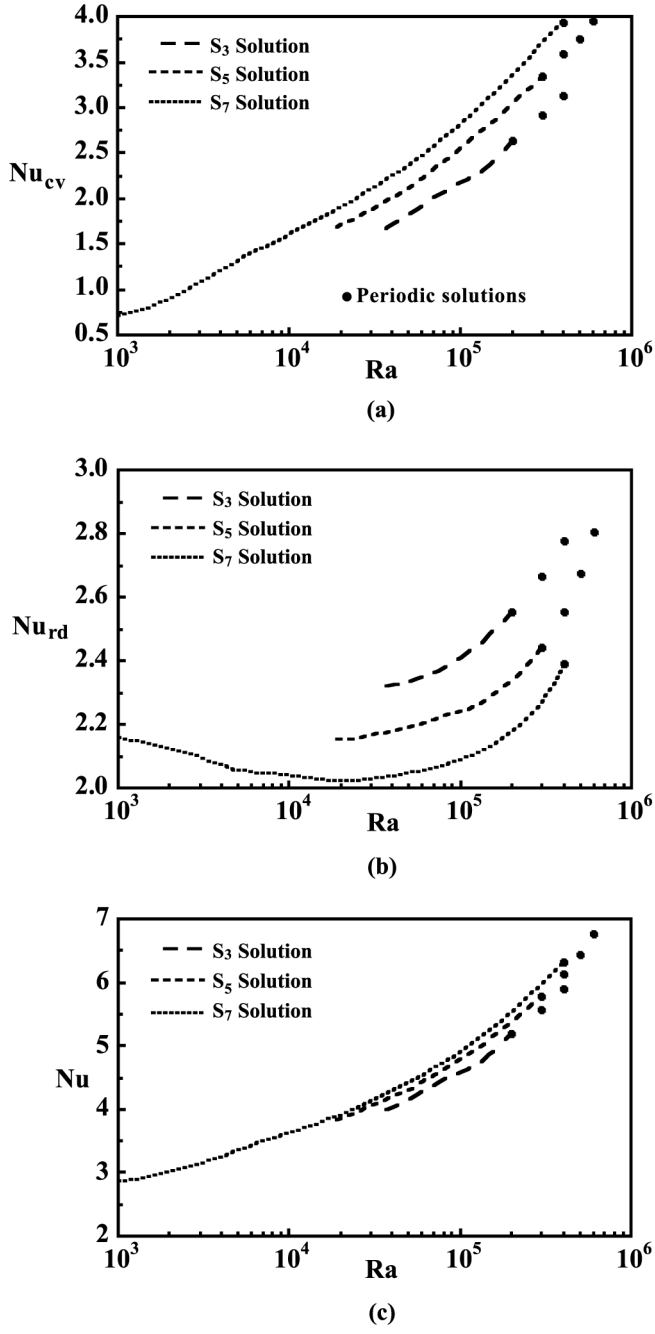

Figure 6.
Variations, with *Ra*, of the average Nusselt numbers on the cold wall of the cavity for $\varepsilon = 0.5$, $\theta = 45°$ and different obtained solutions. (a) Nu_{cv}; (b) Nu_{rd}; and (c) *Nu*

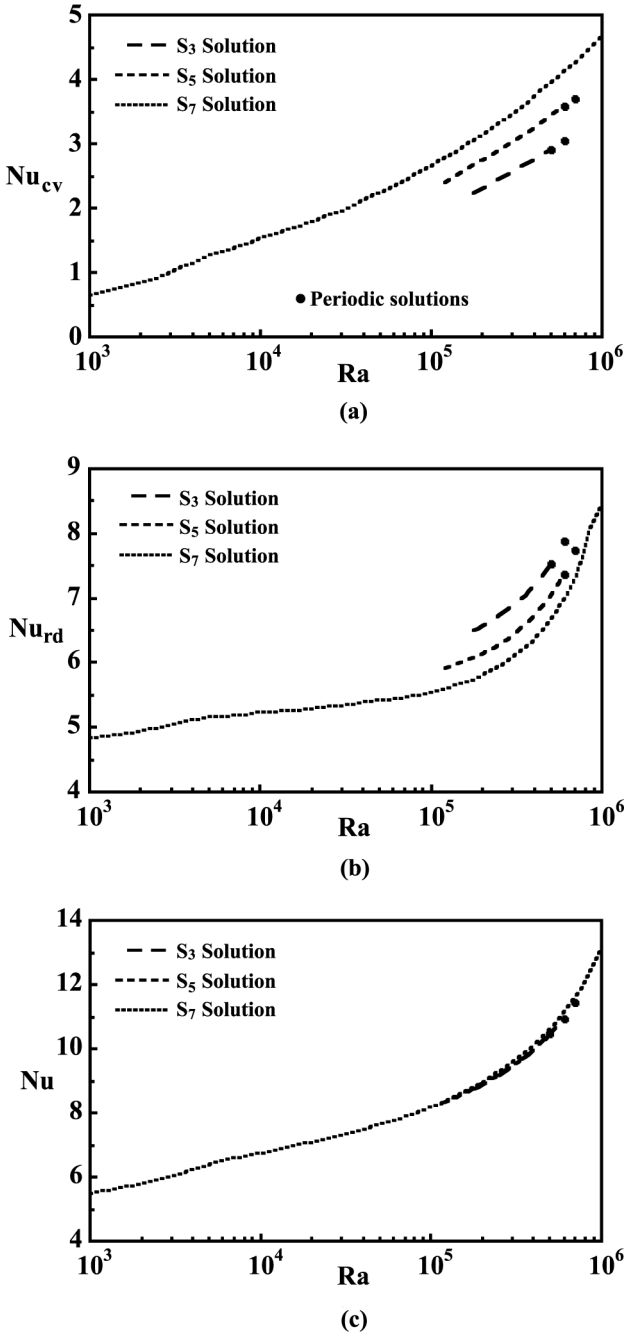

Figure 7.
Variations, with *Ra*, of the average Nusselt numbers on the cold wall of the cavity for $\varepsilon = 1$, $\theta = 45°$ and different obtained solutions. (a) Nu_{cv}; (b) Nu_{rd}; and (c) Nu

shows that the radiation heat transfer is dominant when compared to that of natural convection for all the solutions obtained in the considered range of *Ra*. Variations of the total Nusselt number, presented in Figure 7(c), shows that the increase of *Nu* with *Ra* is monotonous but remains insensible to the type of solution. Finally, it is to underline that *Ra* and ε act on the multiplicity of solutions. In fact, the increase of ε leads to a reduction of the range of *Ra* for which this multiplicity is obtained. Whereas the increase of *Ra* supports the obtaining of the multiplicity of solutions for all the considered values of ε. To be more precise, we present in Table III, the ranges of *Ra* corresponding to the existence of steady solutions of $\mathbf{S}_1$, $\mathbf{S}_3$, $\mathbf{S}_5$ and $\mathbf{S}_7$ types for $\theta = 45°$ and different values of ε.

Case of a vertical cavity ($\theta = 90°$)

In the following sub-sections, the attention is focused on the case of a vertical cavity for which the multiplicity of solutions is not existing.

Streamlines and isotherms. Streamlines and isotherms, illustrating the effect of the emissivity of the walls, are presented in Figure 8(a)-(d) for $Ra = 10^5$ and $\theta = 90°$. Significant changes in the flow structure and temperature distribution are observed when the emissivity of the wall is varied. In fact, in the absence of the radiation effect ($\varepsilon = 0$), Figure 8(a) shows that a great part of the cavity is occupied by a large cell while in its lower part, the fluid is stagnant because of the nature of thermal boundary conditions imposed in this area. The corresponding isotherms show important distortions and are tightened at the level of the heating sources and the upper part of the cold wall which indicates an important heat transfer by convection in these regions from the heating elements to the fluid and from the latter to the cold wall. When the radiation effect is considered, Figure 8(b) shows that, although the considered value of ε is weak ($\varepsilon = 0.1$), its effect is characterized by a trend to generalise the cell movement to the whole space offered inside the cavity. In addition, the radiation effect is favourable to the small vortex located in the vicinity of the upper right corner of the cavity and leads to a contraction of the large cell. The corresponding isotherms show a better homogenisation of the temperature inside the cavity by comparison with the case where the radiation effect is neglected. By increasing the emissivity value to $\varepsilon = 0.5$, Figure 8(c), shows similar structure if we except the upper part of the cavity where the small cell resulting from the radiation effect is more developed and more intense. By increasing ε to its highest value ($\varepsilon = 1$), Figure 8(d) shows that the radiation effect leads to the appearance of another small convective cell at the vicinity of the adiabatic portion, located between the two upper heating sources which causes a reduction of the large cell intensity. This change of the dynamic and thermal structure is due to a significant reduction in the local temperature along the adiabatic walls (Figure 9) engendered by the radiation effect. Consequently, the fluid is decelerated at

Table III.
Ranges of *Ra* corresponding to the existence of steady solutions of $\mathbf{S}_1$, $\mathbf{S}_3$, $\mathbf{S}_5$ and $\mathbf{S}_7$ types for $\theta = 45°$ and different values of ε

Type of solution	$\varepsilon = 0$	$\varepsilon = 0.5$	$\varepsilon = 1$
$\mathbf{S}_1$	$10^3 \leq Ra \leq 5 \times 10^5$	–	–
$\mathbf{S}_3$	–	$3.1 \times 10^4 \leq Ra < 2 \times 10^5$	$1.5 \times 10^5 \leq Ra < 5 \times 10^5$
$\mathbf{S}_5$	$2.8 \times 10^3 \leq Ra < 3 \times 10^5$	$1.9 \times 10^4 \leq Ra < 3 \times 10^5$	$1.2 \times 10^5 \leq Ra < 6 \times 10^5$
$\mathbf{S}_7$	$2.8 \times 10^3 \leq Ra < 5 \times 10^5$	$10^3 \leq Ra < 4 \times 10^5$	$10^3 \leq Ra \leq 10^6$

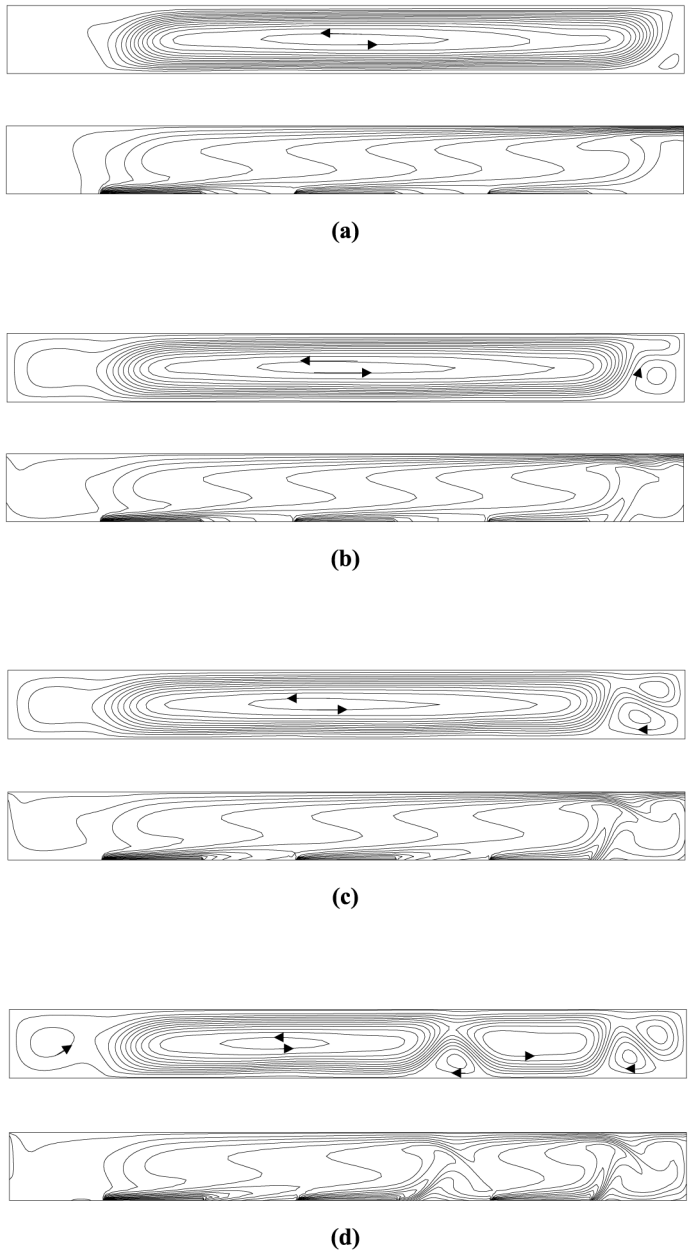

Figure 8.
Streamlines and isotherms obtained for $Ra = 10^5$, $\theta = 90°$ and various values of ε. (a) $\varepsilon = 0$ ($\Psi_{min} = -0.25$, $\Psi_{max} = 53.36$); (b) $\varepsilon = 0.1$ ($\Psi_{min} = -8.56$, $\Psi_{max} = 52.99$); (c) $\varepsilon = 0.5$ ($\Psi_{min} = -12.35$, $\Psi_{max} = 52.52$); and (d) $\varepsilon = 1$ ($\Psi_{min} = -12.88$, $\Psi_{max} = 48.21$)

the level of the adiabatic elements, what favours the formation of a new secondary convective cell.

Effect of ε on the Nusselt numbers. The effect of radiation on mean convective, radiative and total Nusselt numbers are presented, respectively, in Figure 10(a)-(c) for

$\theta = 90°$ and various values of *Ra*. As expected, Figure 10(a), shows that Nu_{cv} decreases by increasing ε for all considered values of *Ra*. More precisely, for $Ra = 5 \times 10^5$, the convective Nusselt number, obtained with $\varepsilon = 1$, is reduced by about 25 per cent when compared to the reference case corresponding to $\varepsilon = 0$. Similar observations, relative to the effect of radiation, were reported in the literature (Balaji and Venkateshan, 1993, 1994a; Akiyama and Chong, 1997). Also, it is to note that, for a given ε, Nu_{cv} increases with *Ra* and the rate of increase is practically independent on ε. For the highest value of *Ra* considered ($Ra = 10^6$), the radiation effect leads to an oscillatory regime characterized by sustained periodic oscillations of the fluid motion. This behaviour can be explained by the competition between the secondary cells, which are supported by the presence of radiation, and the main cell. The values reported in Figure 10(a)-(c) by full circles are obtained for $\varepsilon \geq 0.1$; they correspond to mean values of the periodic solutions characterized by weak periods and amplitudes. Concerning the effect of radiation on Nu_{rd}, Figure 10(b) shows that this effect is more pronounced; the radiative Nusselt number increases quickly with ε and the rate of increase with *Ra* depends on ε. In Figure 10(c), it is seen that the tendency of *Nu* is imposed by that of Nu_{rd} since the contribution of radiation to the total Nusselt number is higher than that of natural convection. The comparative study between the two heat transfer modes (convection and radiation), presented in Table IV, shows that the contribution of the radiation is higher than that of the natural convection for $\varepsilon \geq 0.6$.

Effect of Ra *on the Nusselt numbers*. The variations of the Nusselt numbers with *Ra* are presented in Figure 11(a)-(c) for $\theta = 90°$ and various values of ε. In Figure 11(a), the variations of Nu_{cv} with *Ra* are characterized by a continuous increase for all the considered values of ε. Sustained periodic solutions are obtained for large values of *Ra* in the presence of radiation. Similar phenomenon is observed and discussed in the previous section. For a given value of *Ra*, the natural convection effect decreases by increasing the radiation effect (increasing ε). Similar observations were reported in the past by Balaji and Venkateshan (1993, 1994a) and Akiyama and Chong (1997). In Figure 11(b), it is seen that the increase of *Ra* involves a limited increase of the radiative heat transfer for values of $Ra \leq 2 \times 10^5 / (\leq 4 \times 10^4)$ for $\varepsilon = 0.5/(1)$. Above these thresholds of *Ra*, the increase of the radiative heat transfer with this parameter becomes significant. The variations of the total Nusselt number, presented in Figure 11(c), show increasing tendencies with *Ra* and ε and the positive impact of

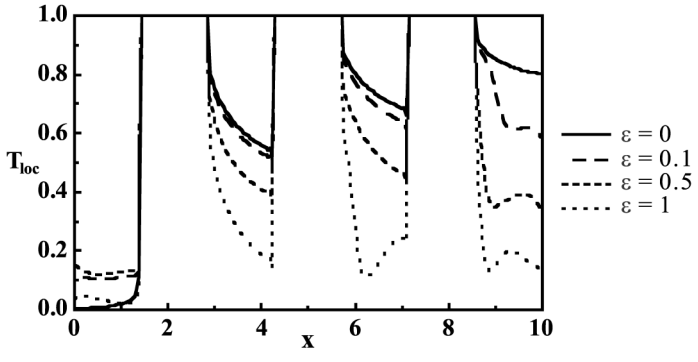

Figure 9.
Temperature profile on the heated wall for $Ra = 10^5$, $\theta = 90°$ and various values of ε

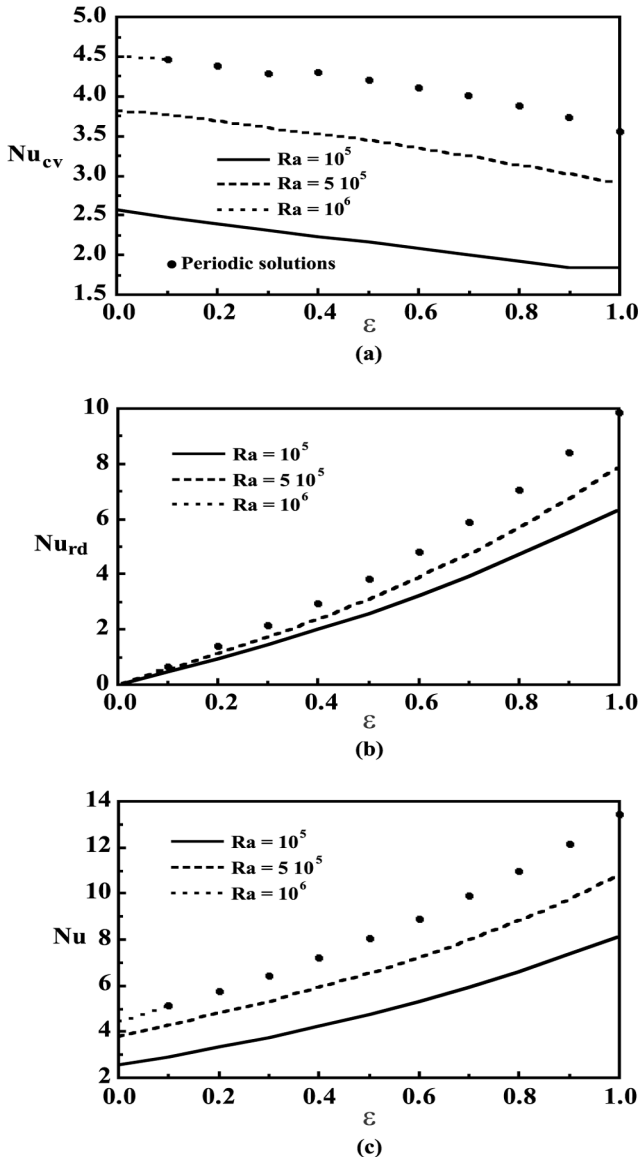

Figure 10.
Variations, with ε, of the average Nusselt numbers on the cold wall of the cavity for $\theta = 90°$ and various values of *Ra*. (a) Nu_{cv}; (b) Nu_{rd}; and (c) *Nu*

Table IV.
Comparison of the convective and radiative heat transfer contributions as a function of ε, for $\theta = 90°$ and various values of *Ra*

	$\varepsilon = 0$		$\varepsilon = 0.2$		$\varepsilon = 0.5$		$\varepsilon = 0.6$		$\varepsilon = 0.8$		$\varepsilon = 1$	
Ra	Nu_{cv}	Nu_{rd}	Nu_{cv}	Nu_{rd}	Nu_{cv}	Nu_{rd}	Nu_{cv}	Nu_{rd}	Nu_{cv}	Nu_{rd}	Nu_{cv}	Nu_{rd}
10^5	2.564	–	2.388	0.940	2.164	2.597	2.088	3.239	1.928	4.702	1.847	6.354
5×10^5	3.826	–	3.683	1.124	3.443	3.100	3.352	3.879	3.146	5.684	2.901	7.889
10^6	4.494	–	4.378	1.388	4.214	3.840	4.117	4.814	3.884	7.074	3.562	9.858

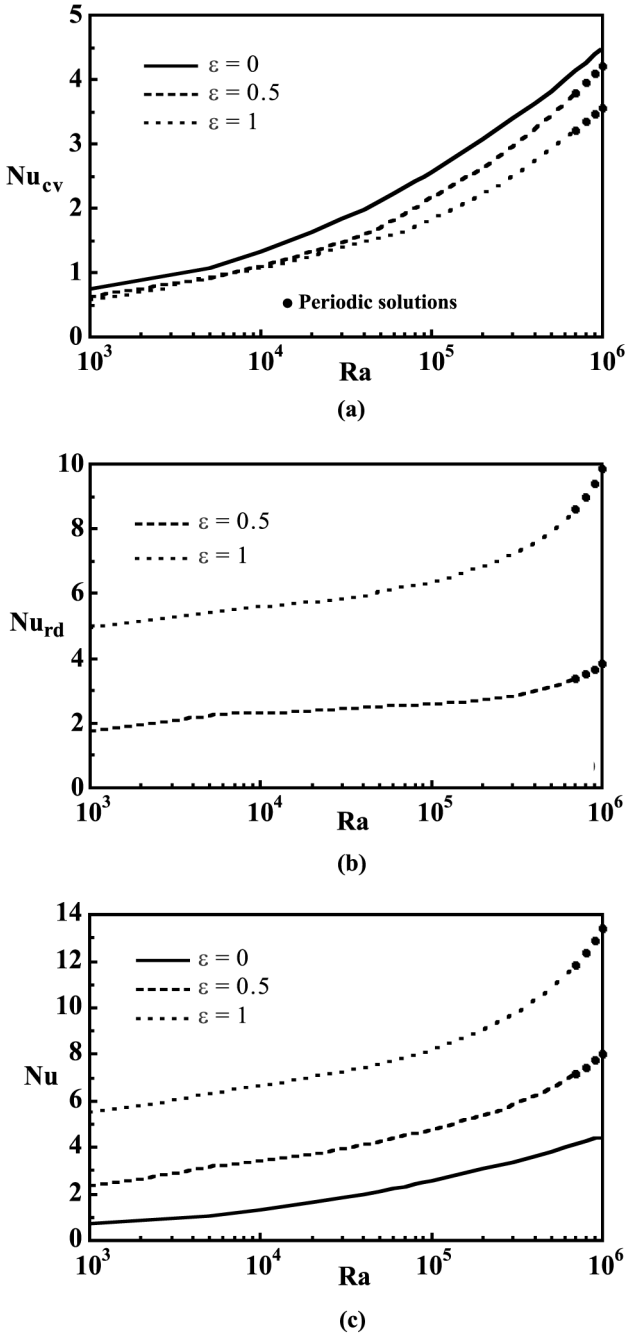

Figure 11.
Variations, with *Ra*, of the average Nusselt numbers on the cold wall of the cavity for $\theta = 90°$ and various values of ε. (a) Nu_{cv}; (b) Nu_{rd}; and (c) Nu

radiation is more important than its negative effect on the convective Nusselt number. A comparison between convective and radiative Nusselt numbers, shows that the contribution of radiation becomes higher than that of natural convection when $Ra \leq 2 \times 10^5/(10^6)$ for $\varepsilon = 0.5/(1)$.

Conclusion

Coupling between natural convection and thermal radiation in a discreetly heated cavity, inclined with respect to the horizontal, was investigated numerically. The results obtained show that, for $\theta = 45°$, up to four different solutions are possible and their appearance depends strongly on the parameters Ra and ε. The increase of Ra favours the multiplicity of solutions for all the considered values of ε. On the contrary, the increase of the latter parameter reduces the number of solutions for weak values of Ra. The solution of $\mathbf{S}_7$ type is found to be the most favourable to the convective and total heat transfer, while those of $\mathbf{S}_1$ or $\mathbf{S}_3$ types are the most favourable to the radiative heat transfer. For the highest value considered for ε ($\varepsilon = 1$), the total heat transfer is independent on the type of solution and for all the obtained solutions, the radiative heat transfer increases by increasing Ra and ε. Even the convective heat transfer increases with Ra, its variation with ε depends both on Ra and the range of ε.

In the case of a vertical cavity ($\theta = 90°$) the radiation effect leads to the appearance of secondary cells for values of $Ra \leq 10^5$. The radiation acts in decreasing the natural convection effect but enhances the overall heat transfer through the cavity. Similar observations were reported in the past about the radiation effect in closed cavities. The introduction of radiation generates periodic oscillatory solutions for large values of Ra which are characterised by weak periods and amplitudes.

References

Akiyama, M. and Chong, Q.P. (1997), "Numerical analysis of natural convection with surface radiation in a square enclosure", *Numerical Heat Transfer, Part A*, Vol. 31, pp. 419-33.

Balaji, C. and Venkateshan, S.P. (1993), "Interaction of surface radiation with free convection in a square cavity", *International Journal of Heat & Fluid Flow*, Vol. 14 No. 3, pp. 260-7.

Balaji, C. and Venkateshan, S.P. (1994a), "Correlations for free convection and surface radiation in a square cavity", *International Journal of Heat & Fluid Flow*, Vol. 15 No. 3, pp. 249-51.

Balaji, C. and Venkateshan, S.P. (1994b), "Interaction of radiation with free convection in an open cavity", *International Journal of Heat & Fluid Flow*, Vol. 15 No. 4, pp. 317-24.

Balaji, C. and Venkateshan, S.P. (1994c), "Combined surface radiation and free convection in cavities", *Journal of Thermophysics & Heat Transfer*, Vol. 8 No. 2, pp. 373-6.

Dehghan, A.A. and Behnia, M. (1995), "Experimental flow visualization of natural convection in discreetly heated open cavities", *Journal of Flow Visualization and Image Processing*, Vol. 2, pp. 209-18.

Dehghan, A.A. and Behnia, M. (1996), "Combined natural convection-conduction and radiation heat transfer in a discreetly heated open cavity", *ASME Transactions*, Vol. 118, pp. 56-64.

Hottel, H.C. and Saroffim, A.F. (1967), *Radiative Heat Transfer*, McGraw-Hill, New York, NY.

Kim, D.M. and Viskanta, R. (1984), "Effect of wall conduction and radiation on natural convection in a rectangular cavity", *Numerical Heat Transfer*, Vol. 7, pp. 449-70.

Larson, D.W. and Viskanta, R. (1976), "Transient combined laminar free convection and radiation in a rectangular enclosure", *Journal of Fluid Mechanics, Part 1*, Vol. 78, pp. 65-85.

Raji, A. and Hasnaoui, M. (1998a), "Mixed convection heat transfer in a rectangular cavity ventilated and heated from the side", *Numerical Heat Transfer, Part A*, Vol. 33, pp. 533-48.

Raji, A. and Hasnaoui, M. (1998b), "Corrélations en convection mixte dans des cavités ventilées", *Revue Générale de Thermique*, Vol. 37, pp. 874-84.

Raji, A. and Hasnaoui, M. (2000), "Mixed convection heat transfer in ventilated cavities with opposing and assisting flows", *Engineering Computations, International Journal for Computer-Aided Engineering and Software*, Vol. 17 No. 5, pp. 556-72.

Ramesh, N. and Venkateshan, S.P. (1999), "Effect of surface radiation on natural convection in a square enclosure", *Journal of Thermophysics & Heat Transfer*, Vol. 13 No. 3, pp. 299-301.

Ramesh, N., Balaji, C. and Venkateshan, S.P. (1999), "Effect of boundary conditions on natural convection in an enclosure", *International Journal of Transport Phenomena*, Vol. 1, pp. 205-14.

Refai Ahmed, G. and Yovanovich, M.M. (1991), "Influence of discrete heat source location on natural convection heat transfer in a vertical square enclosure", *ASME Journal of Electronic Packaging*, Vol. 113, pp. 268-74.

Refai Ahmed, G. and Yovanovich, M.M. (1992), "Numerical study of natural convection from discrete heat sources in a vertical square enclosure", *Journal of Thermophysics & Heat Transfer*, Vol. 6 No. 1, pp. 121-7.

Ridouane, E.H., Hasnaoui, M., Amahmid, A. and Raji, A. (2004), "Interaction between natural convection and radiation in a square cavity heated from below", *Numerical Heat Transfer, Part A*, Vol. 45, pp. 289-311.

Torrance, K.E. (1979), "Natural convection in thermally stratified enclosures with localized heating from below", *Journal of Fluid Mechanics*, Vol. 95, pp. 477-95.

Corresponding author
A. Raji can be contacted at: abderaji@fstbm.ac.ma